

Flight Readiness Report

Midwest Competition 2018

Rocket Team at the University of Minnesota - Twin Cities

Mentor: Gary Stroick, 952-201-3002, president@offwegerocketry.com

Faculty Advisor: Brian Nichols, 612-626-5496, jwn@umn.edu

Student Lead: Jacob Grunklee, 612-231-8773, grunk012@umn.edu

Members: Ryan Thomas, Max Jetzer, Alex Wege,
Wayne Kosak, Paul Gross, Will Busacker, Sophia Vedvik,
Emma Lenz, Anna Cramblitt, Hannah Reilly,
Casey Carlson, Kyle Roberts

May 9, 2018



Contents

1 Executive Summary	4
2 Construction	4
2.1 Airframe	4
2.2 Recovery System	5
2.3 Stability Analysis	6
2.4 Canard Set Mechanical Structure	6
2.5 Fin Design	6
2.5.1 Fin Attachment	8
2.5.2 Aeroelastic Flutter	9
2.6 DREAM	9
2.7 RCS Thruster System	11
3 Electrical Hardware and AV Bay	11
3.1 Roll Control Module	11
3.2 Flight Computer	13
4 Controller	14
4.1 Testing	14
5 Attitude Determination System	15
5.1 Algorithm	16
5.2 Testing	16
6 Flight Performance	16
6.1 Test Flight March 17, 2018	17
6.2 Test Flight May 5, 2018	18
6.2.1 Flight Data	18
6.2.2 Recovery System Performance	19
6.2.3 Coupler assembly	20
7 Pre- and Post-Launch Procedure Assessment	20
7.1 Changes to Av Bay Assembly Procedure	20
7.2 Pre-Flight Procedure Analysis	20
7.3 Post-Flight Procedure Analysis	21
8 Budget	21
9 Communications Challenge	23
9.1 Objective	23
9.2 Hardware Design	23
9.3 Software Design	23
9.3.1 Bonus Challenge A: Reprogramming on the Pad	23
9.3.2 Bonus Challenge B: Flight Data	24
9.3.3 Bonus Challenge C: Flight Math	24
References	24

1 Executive Summary

The 2017-2018 Minnesota Space Grant Consortium Midwest Competition (henceforth “Midwest Competition”) challenges teams to build a high-power rocket with an active orientation-control system. The rocket must fly to 3,000ft and be safely recovered at least twice. In flight, it must be able to hold a constant roll orientation and roll to a series of predetermined compass angles. As a bonus challenge, teams may implement Xbee-based radio telemetry to communicate with the rocket both in flight and on the pad.

To meet these objectives, the Rocket Team at the University of Minnesota Twin Cities has constructed a 68” long, 4” diameter rocket, dubbed “Wolfram Green.” In the test flight, Wolfram reached an apogee of 3,866ft AGL on an Aerotech J540-R and experienced about 13 seconds of actuating time after burnout and before apogee. According to simulations, stability exceeded 1.25 calibers throughout all phases of ascent. The launch vehicle was designed and simulated in OpenRocket.

To actively control roll, pivoting elliptical canards are actuated through a gear set by four independent servo motors. The servos are driven according to a Linear Quadratic (LQ) state-space controller, a type of Linear Time-Varying (LTV) controller. An attitude solution and control outputs are computed in a real-time environment called the Real Time Executive for Multiprocessor Systems (RTEMS), an open-source operating system platform that provides extremely precise timing. The Roll Control Module (henceforth “R/C”) is based on a Raspberry Pi Zero microcontroller.

A second Raspberry Pi Zero serves as Wolfram’s Flight Computer. This microcontroller relays data to and from the ground via a 2.4 GHz Xbee Pro module, actuates a multicolored LED to indicate direction of actuation, and records video via an outward-facing Raspberry Pi Camera Module V2 and a dual mirror system to redirect the field of view. All avionics are mounted in the coupler on a set of custom-printed, stacking PCBs.

As mentioned in the Preliminary Design Report, the R/C is being developed by Rocket Team jointly for Midwest and for the Spaceport America Cup Competition. The goals of the R/C Project include providing team members with hands-on controls experience and developing a working control module. A more detailed overview of the R/C project goals and requirements can be found in [1].

2 Construction

The launch vehicle for the Midwest Competition was designed, optimized, and simulated in OpenRocket. Wolfram Green (pictured at the test launch in Figure 1) will meet competition objectives by its sturdy, canvas-phenolic construction and a dual-deploy recovery system. Final overall dimensions include a 24” lower section housing the motor and drogue, a 12” coupler containing dual sensors packages and an actuating canard set, and a 28” upper section containing the main parachute. Wolfram weighs about 6.1kg with its motor.

2.1 Airframe

Wolfram was originally designed with a 31.25” long upper body section, but the final length is 28”. Several factors were considered before trimming the upper section. OpenRocket Simulations showed that the shorter tube would slightly increase max mach number from mach 0.56 to mach 0.57, and also marginally increase max velocity and



Figure 2: Completed nose weight. The epoxy/shot mixture weights exactly 500g and moves the CG forward by about 3 inches. The threaded rod stuck through is permanently attached, and connects via an eye nut to the shock cord.

max acceleration. Faster speeds are desirable, since they allow the control fins to exert a greater torque for the same deflection angle. Shortening the tube still left space for the main parachute in the upper section. Previously, the decision to have a longer tube was driven by the need to bring the CG forward of the canards without adding excessive mass. However, the R/C module ended up 600g under mass-budget, so additional nose weight could be afforded. The nose weight was increased from 200g to 500g.

Wolfram sports a Wildman wound-fiberglass nose cone. An experimental construction technique was used to add forward nose weight. A plastic icing bag was inserted into the nose as a liner, then an epoxy/led shot mixture was poured in. The resulting mass element weighs 500g, matches the inner profile of the nose exactly, and is easily removable.

After the first test launch, the airframe was successfully recovered and met expectations in terms of both strength and workability. Beveled edges were put on the fins using a router to reduce turbulence during flight. The 1/8" G10 fiberglass fins also held up throughout the test.

2.2 Recovery System

Safety is the emphasis in recovery system design. Wolfram Green utilizes dually-deployed parachutes, with a 24" drogue at apogee and a 60" main at 750 ft AGL. [2] Separation points are at the lower section and nose. A redundant pair of StratoLogger Altimeters trigger ejection charges. Terminal blocks on the bulkheads and internal wiring are used to limit struggles with wiring ejection chargers. The motor ejection charge backs up ejection at apogee. Both parachutes are wrapped in flame-retardant protector sheets when packed in the rocket to prevent melting or burning. Recovery system performance

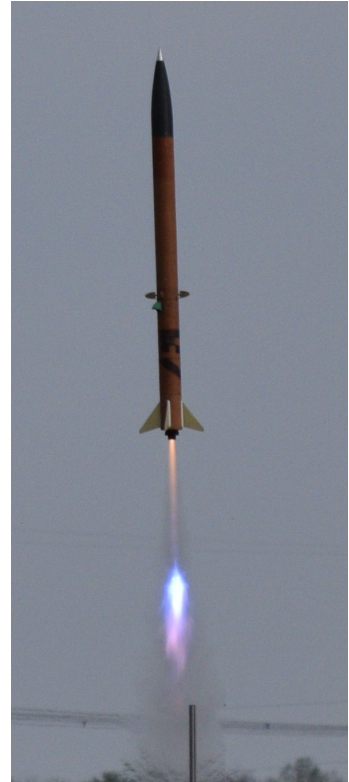


Figure 1: The fully assembled rocket

is discussed in §6.2.

2.3 Stability Analysis

Before the test launch, Wolfram's stability was predicted using OpenRocket. OpenRocket predicts the CG to be 41.7" from the nose and the CP 53.9" back. This results in a stability of about 3 cal. The CG was verified to be within an inch of this at launch. Due to the considerable nose weight added, Wolfram's CG is 3.5" in front of the leading edge of the canard fins. Maintaining this distance was critical to keeping the canard design within competition rules. The margin is much larger than expected due to the R/C module being about 600g under mass-budget.

2.4 Canard Set Mechanical Structure

A gearing mechanism is used to rotate the canards. These are driven by servo motors that are controlled by the R/C electronics stack. A full CAD model can be seen in figure 3. The canards pictured here are of a different geometry than those used for the competition; the Midwest Competition canards are elliptical to provide greater control at subsonic speeds.

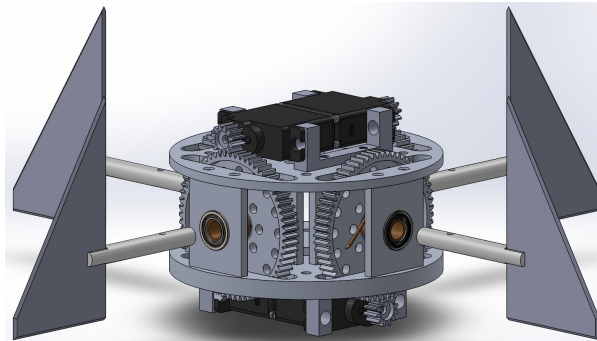


Figure 3: A CAD model of the 4 inch version of the structure.

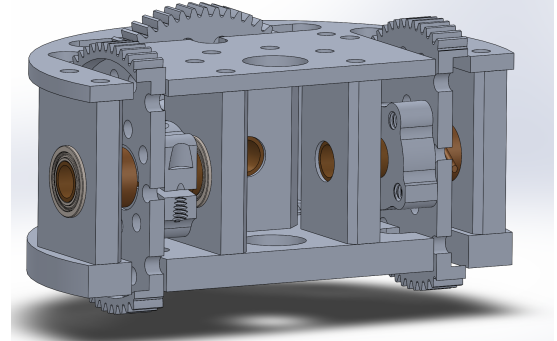


Figure 4: A cut away view of the internals for the 4 inch structure.

This gearing mechanism utilizes 4 servos, one for each canard, in order to minimize the amount of torque needed per servo. The torque per servo is based on the torque analysis done in §2.5. Each servo is attached to a set of gears that further increases the output torque by a factor of 5.33. Utilizing independent servos also reduces the length of the gear train and helps minimize gear slop. Figure 4 shows a cut away of the structure and outlines where the shafts get attached.

An adapter plate is mounted on top of the servos in order to secure the flight computer and the electronics stack. This also houses the screw switches and the camera mount for DREAM. More details about this mounting can be found in §2.6, and [1]. The roll control mechanical structure was hand-machined by students on the team.

2.5 Fin Design

Canards needed to be designed such that they could induce a torque to overcome any disturbance seen past some minimum velocity. Thin airfoil theory and a flat plate assumption was used to determine the coefficient of lift for the airfoil. For the geometry,

an elliptical canard was chosen to maximize the lift for the least induced drag. Then based on work in [3], a relationship between canard area and chord length was determined and a proper size was determined through an iterative process.

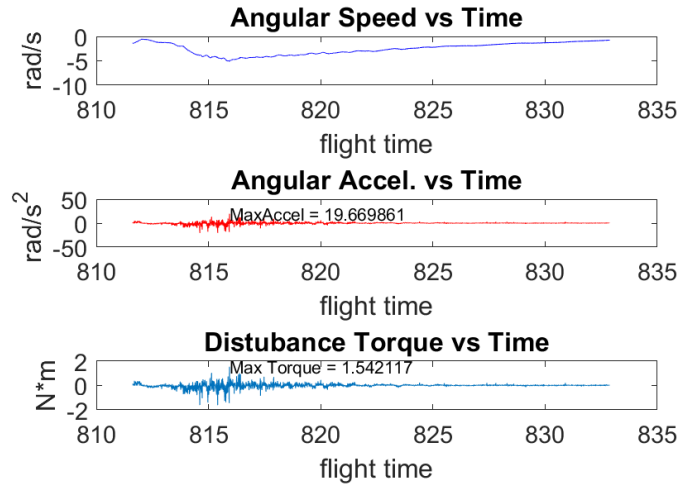


Figure 5: Estimated torque from a 6 inch diameter rocket flight.

Initial estimates of disturbance torques were taken from flight data from previous rockets. Figure 5 shows the measured angular velocity, along with the estimated angular acceleration and maximum torque. These numbers are representative of a 6 inch diameter rocket flight, and it is expected that a 4 inch diameter rocket will experience less torque due to the smaller profile. This can be compared to the simulated disturbance torque of figure 6, as expected the torque on the smaller rocket is much lower.

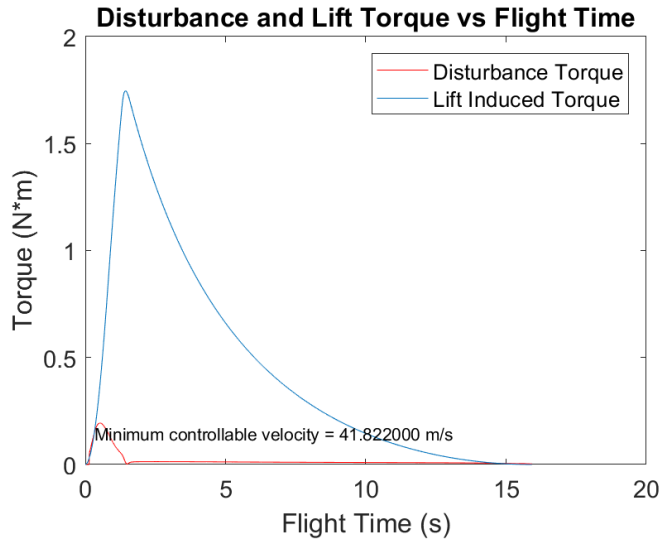


Figure 6: Disturbance torque and canard induced torque for the Midwest Flight as a function of flight time. This is based on OpenRocket simulation data.

Using the newly determined fin dimensions (CAD model of the elliptical fin shown in figure 7), a flight torque profile at maximum fin deflection can be generated and

compared to the disturbance torque. The data used to generate these curves is obtained from OpenRocket Simulations.

Each part of the flight profile is generated using Matlab and the appropriate aerodynamic theory to calculate the total lift produced by the fins. Multiplying the lift force by the moment arm of the fins from the rocket's vertical mass-center gives the torque generated by the canard fins. For Mach less than or equal to 0.3, an elliptical lift distribution and incompressible flow are assumed. This is an especially accurate assumption for the Midwest rocket since each of the canards are half of an ideal ellipse. For Mach in the range of 0.3 to 1.2, the lift coefficient is found using data from fluid simulations and linear interpolation. This is done because the transonic region has proved difficult to characterize through theory alone. The flight torque profile for the Midwest rocket can be viewed below (Figure 6).

2.5.1 Fin Attachment

Since the R/C has been designed to be placed in a coupler, a method for attaching fins needed to be determined. Previously the coupler had large slots cut into the sides; however this severely compromised the structural integrity of the coupler. This led to the design goal of inserting the fins after the rest of the mechanical structure has been inserted into the coupler. It was decided to use set screws to hold the fin shafts in place. This design can be seen in figure 8; it shows a cut away view from the inside of the structure. The set screw goes through a hub clamp, bushing, and the fin shaft. A hub clamp is used to attach the shaft to the gear using screws through the face of the gear.

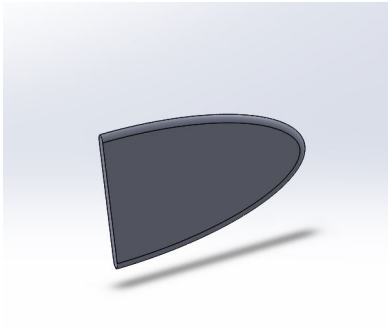


Figure 7: The final fin design for the Midwest rocket

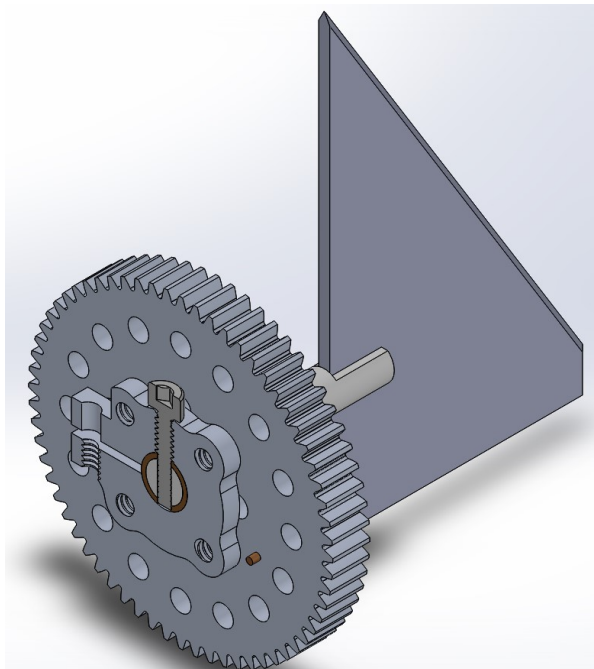


Figure 8: The back view of the fin/gear attachment point.

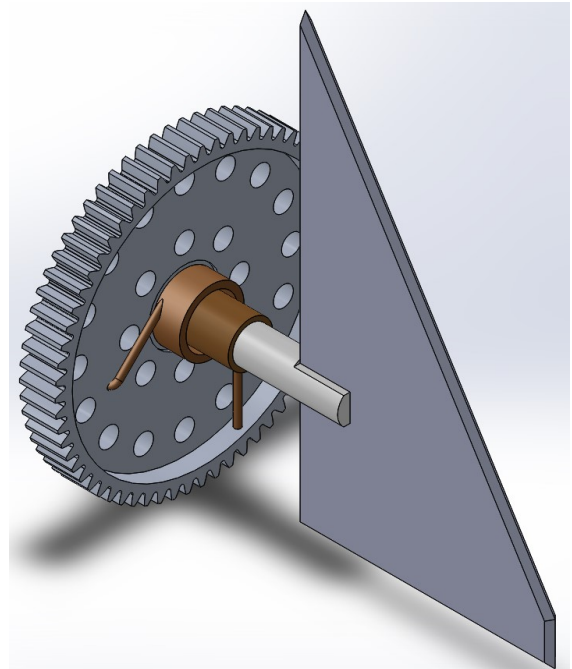


Figure 9: The front view of the fin/gear attachment point with a torsion spring.

This design also allowed for a torsion spring to be connected to the structure and the gear (shown in figure 9). The goal of this spring was to provide constant torque on the gears, thus keeping the gear meshing tight. After testing the R/C without the torsion spring, it was found that the slop was already minimal, and therefore the springs were not needed for the final design.

2.5.2 Aeroelastic Flutter

Fin flutter, or more technically aeroelastic flutter, describes the vibrational mode induced by aerodynamic forces on the fin. There exists a velocity at which air becomes ineffective at dampening the vibration, and the system goes unstable until it eventually breaks apart. A method of calculating this velocity can be found in [4], but the main equation is presented here for completeness (eq 1).

$$v_f = a \sqrt{\frac{2G(AR + 2) \left(\frac{t}{c_r}\right)^3}{1.337P(\lambda + 1)AR^3}} \quad (1)$$

Where a is the speed of sound at the current altitude, P is the pressure at altitude, G is the shear modulus of the fin material, AR is the aspect ratio of the fin, t is the fin thickness, c_r is the root chord, and λ is the ratio of the tip cord to root cord.

OpenRocket was used to generate flight data for air pressure, speed of sound, and flight velocity. This data was then imported into Matlab and ran through equation 1. The results of the simulation are shown in fig 10. As can be seen from the figure, the flight profile lies entirely below the minimum flutter velocity. The figure indicates that flutter will not be encountered during the flight.

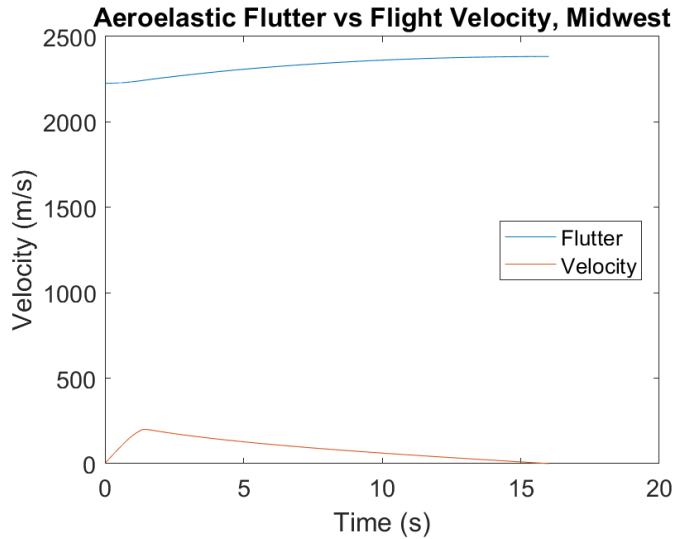


Figure 10: The flight velocity is plotted against the minimum velocity needed to induce flutter for the Midwest Rocket's expected flight profile.

2.6 DREAM

This year's challenge requires the rocket to equip a down-facing camera and monitor control efforts by viewing a set of indicator LEDs. The Dual Reflective Effect of Actuation

Monitor (DREAM) uses a set of two mirrors to ensure all electronics are kept inside the coupler. This is desirable since the flight computer, a Raspberry Pi Zero (see §3), is built to interface with the Raspberry Pi Camera Module V2 via a short ribbon cable. The camera is secured into the mount with screws, with the lens showing through the u-shaped pocket in the mount, and the front surface of the mount is rounded to be flush with the interior of the rocket. The camera mount is attached to the bottom plate of the avionics bay to allow for an easier disassembly process after flight. A CAD model of the mount is shown in figure 11.

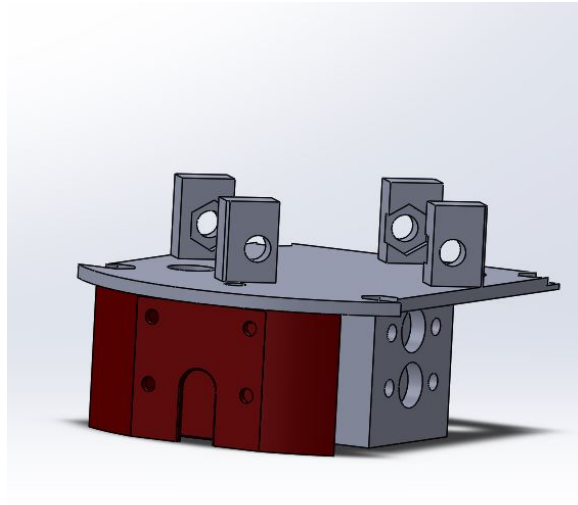


Figure 11: Camera Mount (red) assembled with bottom plate of avionics

The DREAM uses a primary mirror to redirect the field of vision and a smaller secondary mirror to reflect back the image of the LEDs. Both mirrors make 45 degree angles with the rocket. The mount was originally designed to have a length of 3.28", width of 0.57", and protrude 0.6" radially from the rocket. After taking test videos with this design, the field of view was found to be extremely small, so the width was increased to 1.5" and radial dimension to 1.2". Then the distance between the two mirrors was shortened to 0.25".

Ejection tests and the test flight showed that ejection charge debris scratches the mirror surface. Additionally, epoxy was not sufficient to keep the DREAM adhered to the rocket during landing, as the mirror system broke off during the test flight, resulting in a small crack above where the mirror mount had originally been. To reduce the scratching, a clear acrylic window will be placed in the bottom opening of the DREAM. This will block ejection gases from flowing through the mount, preventing scratching. The walls of the mount will also be widened to increase the surface area where it attaches to the rocket. This will help strengthen the lower section and help with adhesion to the side of the rocket.

For the official competition launch, a second DREAM will be prepared in the event that the mount is knocked off during the first flight and another mirror system is needed. Also, a Mobius Action Camera will be placed on the rocket above where the DREAM is mounted. The Mobius will not have a view of the LEDs, but will act as a backup in case the primary camera fails. There have been problems with not having the camera record

in the past, so the backup camera would at least provide footage of the ground and the performance of the R/C canards.

The mirror and camera mounts were designed in SolidWorks and 3D printed in PLA Plastic. The mirrors were laser-cut out of mylar-backed acrylic, placed reflective-side down in the laser cutter in order to prevent safety issues with laser reflection.

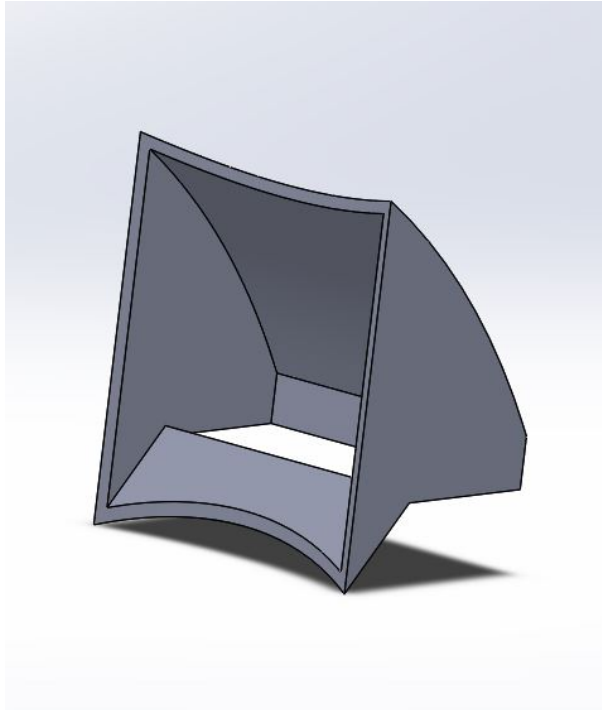


Figure 12: Final Mirror Mount Design



Figure 13: Lab image taken through the DREAM.

2.7 RCS Thruster System

In order to have an alternative actuation method for controlling roll, the team independently developed a compressed-air thruster system. Our planned thruster system would have consisted of high-compressed air being passed through a regulator to bring the output pressure down. From the regulator, the air would have passed through a series of high pressure tubes and splitters to carry air to a pair of nozzle sets, with electronic solenoid valves controlling each set. Due to time constraints and finding that the roll control module consisting of metal fins proved to be a very effective and efficient way to control the roll of the rocket, the construction of the thruster system was no longer continued. The parts purchased to build the thruster might be used by the R/C Project next year.

3 Electrical Hardware and AV Bay

3.1 Roll Control Module

The R/C electronics are designed to sit on stacking printed circuit boards (PCB's) so all the components can fit inside the small diameter coupler, as shown in figure 14. The modular design allows boards to be swapped out if one has a problem. Over several

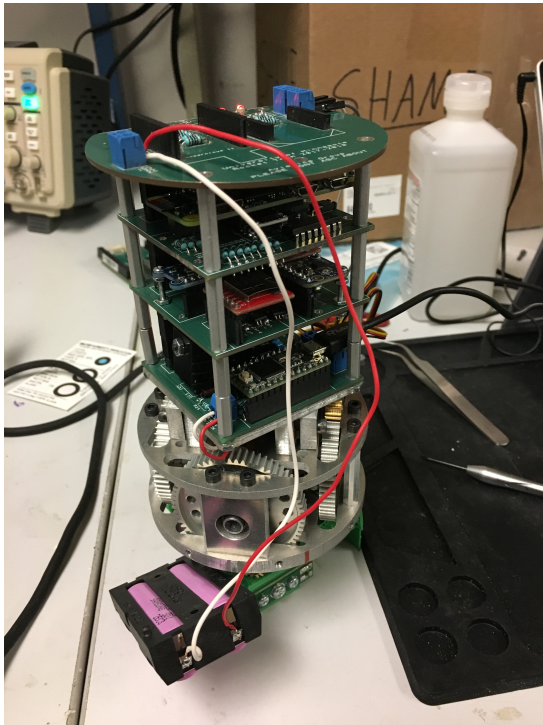


Figure 14: The PCB stack on top of the mechanical structure. The batteries (pink cylinders) are placed on top of the stack when it is inserted into the coupler.

revisions, the back plane connecting the boards remained the same, allowing boards to be interchanged between revisions if necessary (as long as proper software changes take place).

The R/C stack design improves the “user-friendliness” of the AV bay. A stacking PCB design requires only the bottom plate to be attached to the structure before it gets inserted into the coupler. The remaining stack can be attached later. The upper PCB’s plug into the bottom one via a backplane of 2x40 male-female header pairs. This allows for easier assembly and the possibility of accessing the SD card or debugging the boards without needing to remove them from the coupler.

The electronics stack includes the sensors listed in Table 1. The main processing is done on a Raspberry Pi Zero (RPi), but UART communication and servo control are offloaded through a PIC24 microcontroller. The RPi is running a real time operating system called RTEMS in order to maintain strict timing requirements of the controller and attitude determination system. Although a GPS is listed, software restrictions didn’t allow for this sensor to be utilized. Specifically, RTEMS Board Support Package for the RPi does not support UART baud rates that are compatible with those the PIC can generate, preventing data transfer. Given a longer project timeline, work could have been done to read from the GPS over SPI instead of UART, but this would have required an extra electrical component and some additional software work. Repercussions of not having a GPS are briefly explained in § 5

At the test flight, it was determined that the R/C stack still had a physical layout issue that needs to be resolved before competition. Namely, the exposed end of the SD card which stores the operating system and boot files for the RPi ends up pressing firmly against a threaded rod during assembly of the coupler. This resulted in the SD card becoming chipped during the test flight. Revisions are currently being made.

Table 1: R/C Sensor Package

Item	Company	Part #
Magnetometer	Melexis Technologies	LSM9DS1
Accelerometer	Analog Devices	ADXL377
Gyroscope	STMicroelectronics	L3GD20H
GPS	Trimble	Copernicus II
Pressure Sensor	Honeywell	HSCMNNN1.6BAAA3
Temperature Sensor	Texas Instruments	LM61

3.2 Flight Computer

The R/C electronics stack (See §3.1 above) is a generalized device meant to operate during both the Midwest and Spaceport America Cup competitions. An additional pcb mounted in a similar fashion below the mechanical structure will be used to provide Midwest-specific functionality, including radio up- and down-link, video recording, backup datalogging, and auxiliary sensor data collection. This PCB is referred to as the Flight Computer (FC).



Figure 15: First revision of the Flight Computer, not yet populated. The PCB worked electrically but didn't physically fit in its desired place. It was not flown during the test flight for this reason.

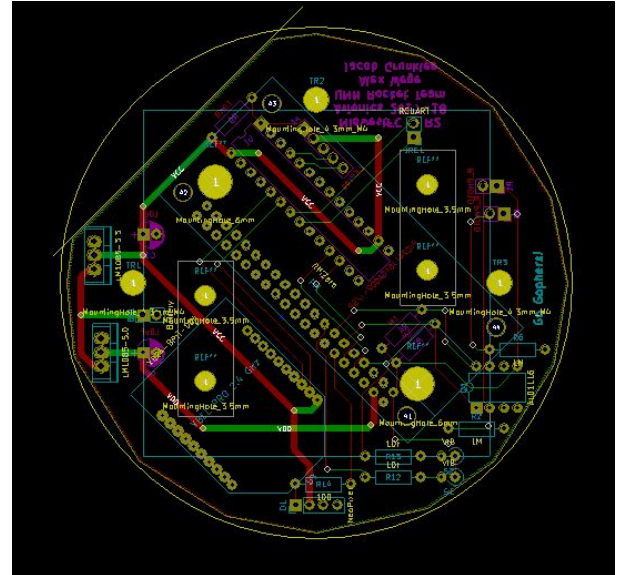


Figure 16: The second PCB revision is still being printed. It resolves the physical space problems encountered in the first revision. Both boards were designed in KiCad and printed by Advanced Circuits.

The preliminary FC PCB (Figure 15) was assembled and tested before the test flight. Electrically, it performs as expected. However, this PCB did not fit properly in the coupler when assembled. This prevented it from being flown and tested during the test flight. A second PCB (Figure 16) is currently being designed and printed that will meet space constraints.

4 Controller

Control theory can be broken into two large categories: frequency domain approaches and time domain approaches. Frequency domain approaches, otherwise known as classical control theory, analyze systems – or plants, as they are commonly referred to – using transfer functions that provide the response due to inputs at different frequencies. Common controllers discussed from this approach include Proportion-Integral-Derivative (PID) and lead-lag. Time domain approaches, also known as modern control theory, consider systems based on the passage of time and are expressed as state-space models in matrices. Controllers in this category often use full-state feedback, or the knowledge of all of the states of the system. It should be noted that all of these controllers can be approached from the other domain, but these are the contexts in which they are most frequently discussed. This project focuses on the time domain approach utilizing a Linear Quadratic (LQ) controller. A complete discussion of this type of controller and the plant dynamics, given by the equations for rotational motion, can be found in numerous textbooks and papers [5, 6, 7].

4.1 Testing

Due to nonlinearity of the spacecraft attitude model, careful consideration must be made to determine robustness to uncertainty. By linearizing the system via a Taylor series expansion, the dynamics change at each time-step. Thus, normal robustness measures using gain and phase margins become more difficult for smaller time-steps. Therefore, robustness in uncertainty using Monte Carlo simulations and polytope visualizations were explored. To determine domains of attraction (regions of stability of the system), the initial conditions were initialized in a uniform distribution of $[-3, 3]$ for angular velocity and $[-\pi, \pi]$ for Euler angles. For one Monte Carlo simulation, one controlled trajectory is determined using the random initial conditions. To determine stability, a comparison between the reference and the state is made to check for convergence to a tolerance. If it converged, the initial condition is saved to produce a polytope which contains the region of stability.

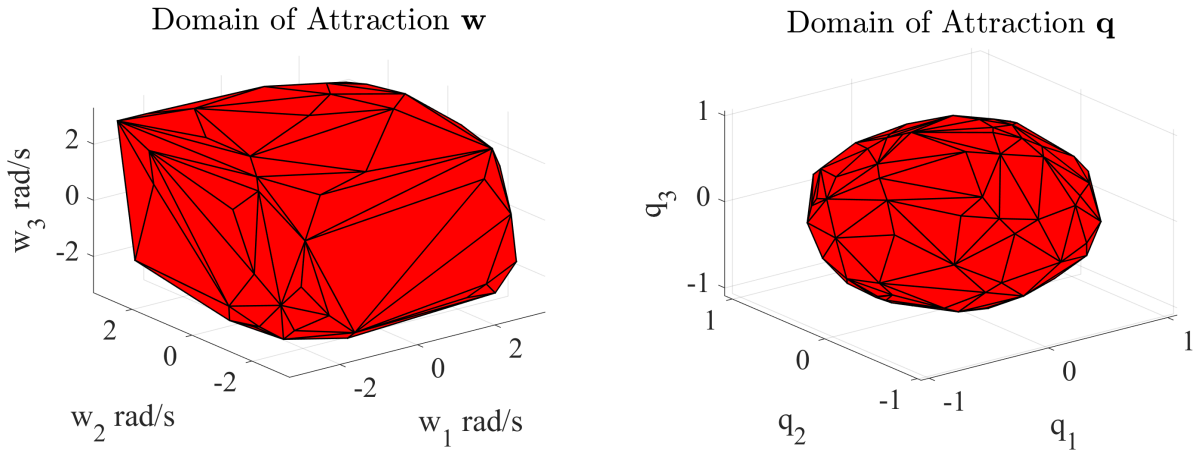


Figure 17: This outlines the domain of attraction for various initial angular rates.

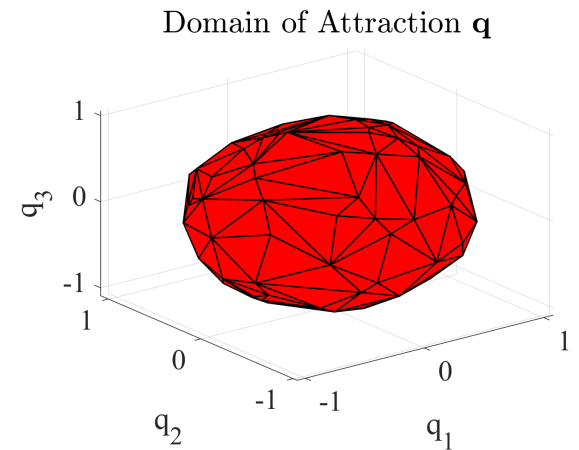


Figure 18: This outlines the domain of attraction for various initial attitudes.

Figures 17 and 18 show the domain of attraction for angular velocity and quaternions

for 1000 Monte Carlo simulations. For angular velocity, the controller can stabilize up to $\pm 2\text{rad/s}$. This provides robustness for high angular rates in every direction. For quaternions, the domain of attraction takes a significant portion of the quaternion space. Note that q_1 is not shown since it is assumed to be constant. Quaternions are also normalized between $[0, 1]$, and from the plot, the controller is robust in variation of the initial conditions for quaternions. These simulations and plots were conducted in Matlab.

5 Attitude Determination System

The controller was designed assuming full state feedback, but because sensors that directly measure attitude are not available an estimator must be designed. The algorithm intended to be used here is a typical fusion of Global Navigation Satellite System (GNSS), and Inertial Navigation System (INS) using an extended Kalman filter. A detailed explanation of the algorithm can be found in [8], and a description of Kalman filtering techniques is given in [9]. This type of system was chosen because of the high accelerations seen by the rocket. Other algorithms such as [10] use vector matching and work well in applications that do not experience large accelerations. These algorithms are an improvement over simple integration techniques because they account for the measurement noise, and reduce the effect of the drift rate of the gyroscopes. However, due to software limitations in obtaining GPS measurements a simple integration method is used instead of the more sophisticated GNSS/INS filter.

The attitude is represented as a set of quaternions to stay consistent with the controller. This also improves computational efficiency and in general, avoids singularities. The integration method utilizes gyroscopes to obtain the rotation rate of the body with respect to the inertial frame. Since the flight time is short it is assumed that the rotation of the navigation frame with respect to the inertial frame is negligible thus the gyroscope measurements can be used directly.

A detailed description of using gyroscopes to integrate quaternions can be found in [11]. Throughout this work it is assumed that the scalar part of the quaternion is the first term in the vector. This algorithm requires an initial estimate of attitude in order to correspond to the correct reference frame. Since the controller utilizes the NED frame, the initial attitude is also computed relative to the NED frame. This initial estimate could be obtained through a vector matching solution performed during the startup procedure of the software. However, this would require a magnetometer calibration routine and wasn't implemented due to time constraints. This is possible since the initial orientation of the rocket is given in the rules, but a brief summary of the vector matching routine is given here for completeness.

First the body frame matrix is constructed using normalized measurements from the accelerometer and magnetometer, equation 2.

$$B = [\bar{\mathbf{m}}^b, \bar{\mathbf{f}}_{ib}^b, \bar{\mathbf{m}}^b \times \bar{\mathbf{f}}_{ib}^b] \quad (2)$$

Then the inertial matrix can be constructed using the normalized gravity vector in the NED frame, and the normalized magnetic reference field in the NED frame, equation 3.

$$N = [\bar{\mathbf{m}}^n, \bar{\mathbf{g}}^n, \bar{\mathbf{m}}^n \times \bar{\mathbf{g}}^n] \quad (3)$$

Then the DCM can be obtained by solving $N = C_b^n B$ for the DCM C_b^n (equation 4). However, the quaternion desired is a transformation from the NED to the body fame. So knowing $C_n^b = C_b^{n^{-1}} = C_b^{n^T}$ the quaternion can be extracted from the DCM.

$$C_b^n = NB^{-1} \quad (4)$$

5.1 Algorithm

The attitude of the rocket can be described by equation 5, where $\omega(\hat{\mathbf{q}})$ is a matrix of the previous quaternion. This equation neglects the rotation rate of the earth and uses the gyroscopes directly.

$$\dot{\hat{\mathbf{q}}} = \frac{1}{2}\Omega(\hat{\mathbf{q}})\hat{\omega}_{ni}^b \quad (5)$$

This solution doesn't account for sensor noise and the integration error continues to build up. Eventually the attitude solution will become corrupt and no longer usable. However, this depends on the quality of sensors used. For many commercial MEMS gyroscopes, such as those used in this project, the bias drift rate is on the order of a few degrees per hour and since the flight time is much less than an hour a usable solution is achievable. Another way of mitigating errors is to implement a take off detection system that only propagates the attitude once the rocket starts acceleration.

The launch detect is based on velocity, which is found by a simple integration of accelerometer measurements. To mitigate the effect of noise, a minimum acceleration is necessary before the velocity integration occurs. This minimum acceleration acts as a noise floor, but has the detrimental effect of delaying the velocity, and thus attitude observations.

5.2 Testing

Testing was conducted on hardware to verify tip over detection and proper orientation sensing. This was done by observing the calculated euler angles in real time while rotating the electronics stack. The results appeared to visually track the expected outcome. More sophisticated hardware in the loop testing could be performed, but due to time constraints and a lack of proper equipment (hardware and software) these were not done.

Software in the loop testing was also not performed since the performance greatly depends on the measurement noise, and the equation to be implemented is straight forward. Flight performance is discussed in a later section.

6 Flight Performance

In order to verify the simulation results and prepare for the competition, several test flights were conducted. Due to time and monetary constraints, an iterative test launch sequence couldn't be completed. Instead, multiple attempts at a controlled test flight were made. Prior to each flight a code review was conducted to ensure the system was in a flight ready configuration. Post launch data analysis was done and the results were used to improve the system before the next test.

6.1 Test Flight March 17, 2018

A test flight was conducted on March 17, 2018. At this time, the competition rocket was not completely flight-ready, so the R/C system was flown on a designated test rocket, designed, purchased, and built by the R/C Project. Since the test rocket does not effectively belong to the Midwest Competition team, it is not included in the budget. This launch used revision 1 of the R/C PCB stack and a minimal version of the state machine and attitude determination system. Due to issues with some surface mount components, some of the non-critical sensors were unavailable. Also, data transmission to the ground station wasn't utilized on this flight.

A bug in the SD card initialization caused the on board logging to fail, and a malfunction with the video camera resulted in no video footage. However, an AIM XTRA was flown as a redundant data collection device. This resulted in the data shown in figures 19 20 and 21.

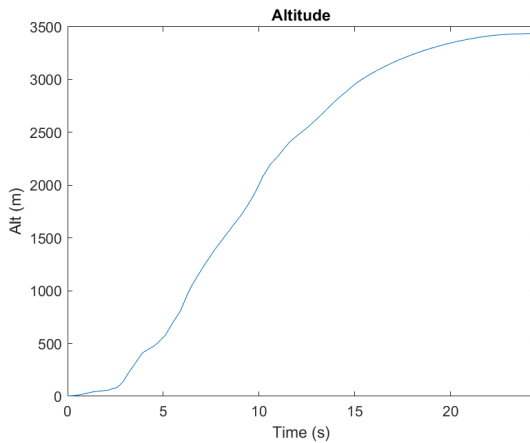


Figure 19: The altitude achieved as measured by the AIM XTRA.

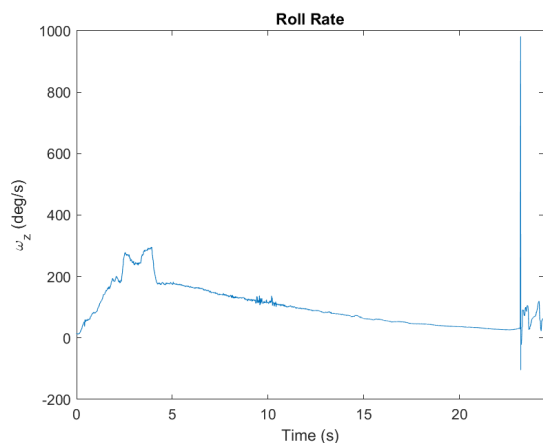


Figure 20: The roll rate as measured by the AIM XTRA.

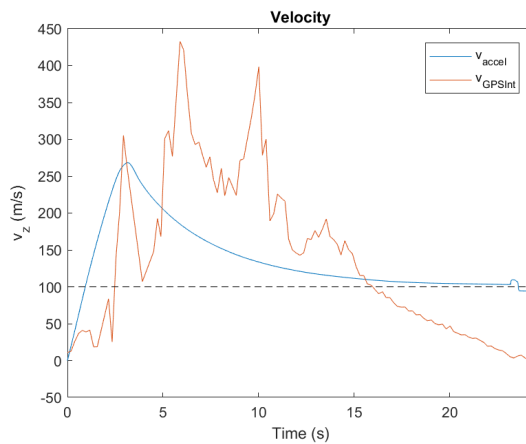


Figure 21: The vertical velocity as estimated from accelerometer and GPS altitude measurements on the March 17, 2018 test flight. The dotted line is the minimum controllable velocity.

Figure 19 gives an idea of where in the flight certain events happened, and shows the total altitude achieved during the flight. Since velocity wasn't directly measured,

estimates were obtained from integrating the altitude from GPS measurements. However, the GPS has a slow update rate so the acceleration estimates from this are noisy. Accelerometer measurements were also used to obtain an estimate of velocity. But this failed to properly account for gravity so this estimate is also not ideal. But when plotted against the minimum controllable velocity, as in figure 21, an estimate for the controllable regime can be obtained. As shown in figure 20, no noticeable change in roll rate can be observed around the time of transitioning to the controllable regime. This could be due to the controller failing to calculate the correct gain, or it could be from the fin size being incorrect. Another possibility is the on-board estimates reached the end parameters before they should have causing the system to go into its end state. The decrease in roll rate is attributed to typical conditions seen after motor burn out. This is based on observations from prior flights with other rockets that lacked canards, or a control system.

Upon recovery, an ejection charge was found to have not gone off but the corresponding shear pins had been sheared. This could have been because the controller was applying a torque on the rocket, which caused the pins to shear. It has been hypothesized that only using 2 shear pins was the cause of this failure and more pins will be used on future flights. If the pins sheared in flight, this would have allowed for the half of the rocket with the roll control module to spin independently of the half with the AIM XTRA.

Although there were several issues with this test launch, there were still lessons learned from it. The data logging needed more testing in order to ensure that it would be successful during flights. More shear pins were necessary to avoid shearing pre-ejection. The subsystem did not pose a threat to overall rocket stability or structural integrity. While the subsystem didn't succeed, it also didn't noticeably fail. Because of a lack of evidence showing the controller diverged, it is assumed that the controller attempted to actuate, but the state machine caused a shutdown before the roll rate could be affected.

6.2 Test Flight May 5, 2018

On May 5th 2018, a test flight using the competition rocket was done. Due to time constraints, Wolfram was launched only one time with the R/C. Wolfram was successfully recovered from this flight, as was the R/C. Unfortunately, due to unexpected software bugs, the team was forced to choose between logging flight data and actuating the canard fins. Actuation was chosen, on the grounds that the camera would capture sufficient data. However, the camera did not record video either, a result of the failure of the first revision of the flight computer to fit in its place in the coupler. The temporary flight computer flown in its place simply did not secure the camera cable well enough.

As a result, the best data available is from the Stratologger altimeters, which will be used extensively in the following analysis. Due to limited motor selection at the launch, Wolfram Green was flown on a J540 motor instead of a J800. This was the motor with the most similar total impulse available at the time of the launch. The desired motors will be available at the competition.

6.2.1 Flight Data

From the Stratologger within the rocket, the altitude data was easily obtained. Wolfram hit apogee at 3,866ft, approximately 13 seconds time between burnout and apogee. Figure 22 shows the data retrieved from the Stratologger. This data matches the Open-

Rocket simulations well; simulated apogee on the J540 was 3806ft, again with 13 seconds of coast time.

Flight Profile

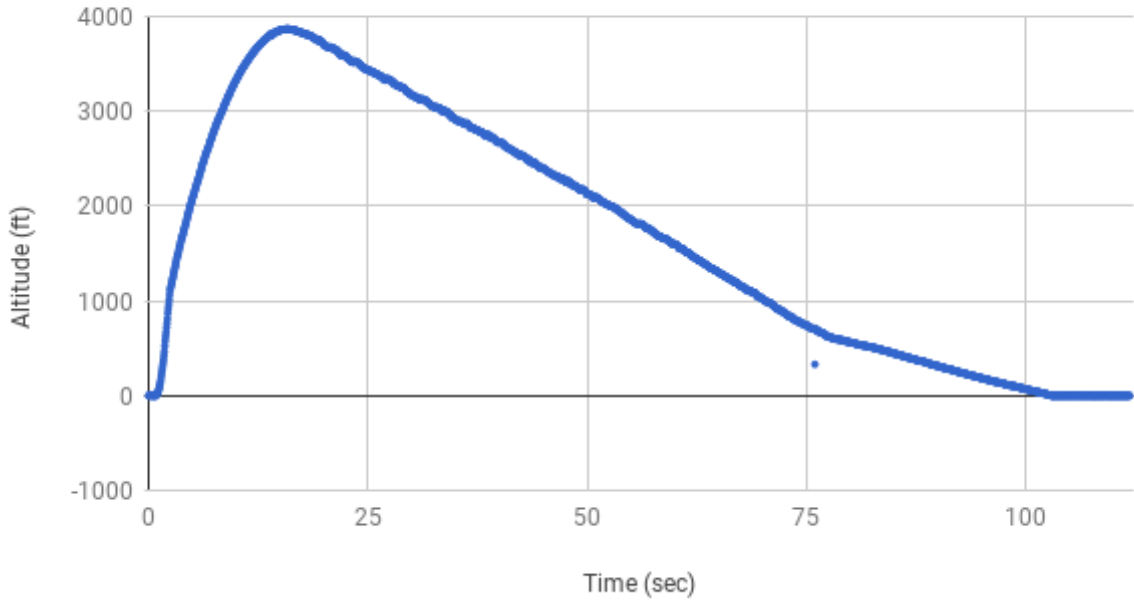


Figure 22: Altitude of the rocket based on data received from working Stratologger

Since velocity was not directly measured during this flight, approximations were made from taking the derivative of the Stratologger altitude data. The simulated max velocity on the J540 was 167m/s with a max acceleration of 102m/s². However, the “actual” max velocity was 268m/s with a max acceleration of 275m/s². This approach is rough, but as mentioned it is the best data available. Better data will be logged during the competition once the second revision of the flight computer is completed.

6.2.2 Recovery System Performance

At the test flight before approaching the launch rail, both Stratologgers were turned on and indicated that all ejection charges had continuity. However, only one altimeter turned on after the rocket was loaded on the launch rail. In the interest of time, the team as a whole decided to fly with a single altimeter. This altimeter performed flawlessly, ejecting the drogue at apogee as expected and successfully ejecting main at 750ft.

Based on OpenRocket Simulations, the expected descent rate under drogue was 20m/s and 7.35m/s under main. Based on the derivative of the Stratatalogger data, the actual descent rate under drogue was 16.3m/s and 7.65m/s under main. This means impact velocity is about 25.1ft/s, slightly higher than the 24ft/s constraint imposed by the competition rules. To decrease descent speed under main, a larger main parachute will be employed at the competition.

6.2.3 Coupler assembly

The test flight showed that one of the biggest remaining design challenges is in making the coupler efficient to assemble. The wires passing through to and from either altimeter, as well as the wires from the screw switches, made the stack assembly more difficult than expected. A temporary “flight computer” had been scrapped together for the purpose of simply recording video during this launch. However, its hasty design proved extremely difficult to assemble, which further delayed overall assembly. While the latter problem will not occur at competition, a wire-management strategy still needs to be implemented.

7 Pre- and Post-Launch Procedure Assessment

7.1 Changes to Av Bay Assembly Procedure

As mentioned in §6.2.3, assembling the coupler was much more difficult and time-consuming than expected. Several steps will be taken during the competition to ensure that this procedure is simpler and mostly complete before arriving at the launch field.

1. The R/C mechanical core will remain assembled from the test launch, since no changes need to be made to it.
2. The upper and lower connection plates will be completely pre-assembled.
3. Servo wires will be shortened. Power and ground wires will be pre-spliced down to a single wire that actually fits in the terminal blocks.
4. The flight computer will have set-screw access holes that allow it to be mounted outside of the coupler. This also reduces stress on the camera cable and allows it to be plugged in from outside the coupler.
5. Altimiter wiring will be labeled and cut with excess length, to be trimmed to fit during assembly.
6. Care will be taken during PCB re-design to leave space for the threaded rods that hold the coupler together.

On the other hand, some aspects of the coupler design, such as the cross-sectionally mounted roll control mechanical structure and the R/C electronics stack, were very easy to assemble and do not need significant changes. Taking video and/or data off of the flight computer after flights will also be relatively easy, since the RPi is easily accessible upon opening up the bottom of the coupler.

7.2 Pre-Flight Procedure Analysis

At the test flight, the pre-flight procedure described in the PDR [1] was followed closely and effectively ensured a safe and thorough launch. The single exception was the lack of use of a radio beeper to track the rocket after liftoff. A radio beeper will be used at competition, to be inserted in the rocket at the same time as the main parachute and shock cord.

7.3 Post-Flight Procedure Analysis

Since the test flight did not require immediate preparation for a second launch or the extraction of data from the flight computers, the procedure followed was slightly different. Important safety items, such as powering off electronics and disconnecting unused ejection charges were done. Post-launch pictures, damage inspection, and data retrieval were conducted thoroughly after returning to the lab.

8 Budget

Item	Cost	Quantity	Subtotal
Flight Computer			
Xbee Pro 2.4GHz	\$32.00	4	\$128.00
12"x12" acrylic-mylar mirror	\$8.99	1	\$8.99
Raspberry Pi Zero	\$5.00	2	\$10.00
RPi v2 Camera Module	\$29.99	1	\$29.99
Roll Control Electronics			
Screw switches	\$2.95	6	\$17.70
Blue LED	\$0.52	25	\$13.00
Red LED	\$0.39	25	\$9.75
Green LED	\$0.52	25	\$13.00
Gyro	\$12.50	1	\$12.50
Xbee Headers	\$0.95	3	\$2.85
Tall back plane headers	\$2.95	20	\$59.00
RPi headers	\$1.50	2	\$3.00
Mag	\$14.95	3	\$44.85
Micro SD card headers	\$3.95	2	\$7.90
5/8" standoffs	\$0.56	25	\$14.00
1" standoffs	\$0.60	40	\$24.00
3.8K Resistor 1/4 W Axial	\$0.10	10	\$1.00
Right angle headers	\$5.53	3	\$16.59
Pressure sensor	\$35.48	3	\$106.44
2x20 Male Headers	\$0.71	15	\$10.65
LM1085 ADJ	\$1.92	5	\$9.60
12 Bit ADC	\$2.82	10	\$28.20
1K Resistors 1/4 W Axial	\$0.10	100	\$10.00
1M Resistors 1/4 W Axial	\$0.10	50	\$5.00
Battery Holder	\$4.48	2	\$8.96
Heat Sinks	\$0.21	10	\$2.10
Backplane TFSM	\$2.95	5	\$14.75
SMA Crimp Connector	\$2.23	2	\$4.46
2Pin Jumper	\$0.10	10	\$1.00
4-40 Screws (3/8)	\$1.60	1	\$1.60
4-40 Screws (5/8)	\$2.10	1	\$2.10
6-32 Nuts	\$1.24	1	\$1.24
Teensy 3.2	\$19.80	3	\$59.40

Copernicus II	\$74.95	1	\$74.95
Standard Female Headers	\$1.50	10	\$15.00
GPS Antenna	\$12.95	1	\$12.95
18650 Battery	\$6.90	8	\$55.20
18650 Charger	\$13.00	2	\$26.00
6-32 Threaded Rod	\$3.89	2	\$7.78
<hr/>			
Roll Control Structure			
Belleville disc spring , (94065K26)"	\$2.70	1	\$2.70
Torsion spring , 90 deg.(9271K584)"	\$5.01	2	\$10.02
Metal for machined parts	\$83.00	1	\$83.00
Hub gear , 32P , 64T(615194)"	\$12.99	4	\$51.96
Face tapped clamping hub (545592)"	\$5.99	4	\$23.96
Flanged ball bearing (535046)"	\$1.99	5	\$9.95
HS-82MG Servo(32082S00)	\$19.99	4	\$79.96
32P/24T C1 Spline Servo Mount Gear(615274)	\$14.99	4	\$59.9
<hr/>			
Launch Vehicle			
57" long x 3.9" diameter phenolic body tube	\$80.00	1	\$80.00
10" long x 3.9" diameter phenolic coupler	\$13.00	1	\$13.00
Wildman 4in nose cone	\$69.00	1	\$69.00
12" long x 3.9" diameter fiberglass coupler	\$2.60	1	\$31.20
G10 fiberglass sheet	\$30.00	1	\$30.00
Icing bags	\$7.99	1	\$7.99
1/4" Eye nut	\$2.25	1	\$2.25
Rail guides	\$12.95	2	\$25.90
<hr/>			
Propulsion			
54mm forward closure	\$45.00	1	\$45.00
54mm phenolic motor mount	\$17.35	18"	\$17.35
Aerotech J800T motors	\$67.99	4	\$271.96
54mm phenolic motor mount	\$17.35	18"	\$17.35
54mm motor retainer	\$29.00	1	\$29.00
<hr/>			
RCS Thruster Supplies			
Ninja 45/4500 air tank and regulator	\$199.95	1	\$199.95
Solenoid valves	\$162.65	2	\$325.30
1/8" FFF Tee	\$15.00	5	\$75.00
ASA (paintball) to 1/8" adapter	\$24.95	1	\$24.95
25ft Polyethelyne tubing	\$3.75	1	\$3.75
5220K64 Male compression fittings	\$2.22	26	\$57.72
LiPo Batteries	\$5.50	2	\$10.99
Battery connectors	\$6.49	1	\$6.49
Electromechanical relay (option 1)	\$1.73	2	\$3.46
Solid state relay (option 2)	\$7.27	1	\$7.27
<hr/>			
General			
Competition Fee	\$400.00	1	\$400.00
Lodging	\$600.00	3	\$600.00
Van Rental	\$416.00	2	\$416.00
Shipping	~\$100.00	1	~\$100.00
Grand Total			\$3,776.52

In comparison to the budget made in the Preliminary Design Report (PDR) [1], there is little change. This is due to the fact that most purchases regarding the airframe of the rocket, the electronics of the R/C, and the mechanical structure of the R/C had been made by the time of the PDR. The biggest difference is the purchase of the RCS thruster supplies, which was purchased after the PDR was submitted, but before the reliability of the metal canard roll control system had been tested. The RCS thruster supplies are no longer in use by the Midwest team this year, but will potentially be used by other groups on the rocket team, or by next year's Midwest team.

9 Communications Challenge

9.1 Objective

This year's special communication challenge requires incorporation of a 2.4 GHz XBee Pro radio module on the non-commercial sensor suite. Rocket Team will implement at least two of the three given communication challenges, namely B) transmitting orientation information to a ground station while the rocket is in flight, and C) sending commands and receiving replies from the rocket during flight. As of now Challenge A), which involves reprogramming new orientation instructions to the rocket while it is on the pad, seems unlikely to be implemented in time for the competition.

9.2 Hardware Design

The 2.4GHz Xbee Pro Module is available in two main versions, one which supports WiFi mesh networks and one supporting only point-point or point-multipoint communication. For simplicity, the point-point Xbee Pro Module was selected. This module was also cheaper. The flight computer (as opposed to the roll control module) handles all bonus challenge tasks. This device consists of a Raspberry Pi Zero microcontroller. The Xbee, Pi and other flight computer sensors are mounted to a single custom-printed circuit board. These sensors alone are not sufficient to accurately determine rocket attitude, so the flight computer receives attitude and roll data from the roll control module via a wired UART connection.

9.3 Software Design

9.3.1 Bonus Challenge A: Reprogramming on the Pad

In order to implement this challenge with the current electronics setup, new orientation instructions would have to be sent from the ground station to the flight computer, then forwarded to the R/C electronics stack. Since both computing units have their own PIC microcontroller for communication port expansion, the process is perhaps unduly complicated. Complexity, time constraints, and unexpected bugs with the RTEMs executive make it unlikely that this portion of the bonus challenge can be implemented in time for the competition.

9.3.2 Bonus Challenge B: Flight Data

Fortunately, Bonus Challenge B remains feasible. Flight data will be broadcast from the flight computer to a ground station throughout flight. To improve the efficiency of the data transmission, flight data will be sent to the ground as binary packed data with a single delimiting word at the beginning of each packet. Packets will be about 74 bytes long and will include the delimiting word, the security code, flight status, separation status, altitude, temperature, acceleration, mangetometer, and gyroscope readings. The binary data will unpacked on the ground after the flight completes. The flight computer will log a duplicate copy of the data for comparison.

9.3.3 Bonus Challenge C: Flight Math

The process described in the Preliminary Design Report[1] to send a simple equation to the flight computer, have it calculate the equation, and have it send the answer back to ground station was implemented successfully for the flight computer. This process involved packing each 5-byte math instruction in 2 bytes of data, and prepending a security code to complete the uplink packet structure.

References

- [1] R. T. at the University of Minnesota, “Preliminary design report.” ”Preliminary Design Report for the 2017-18 Midwest Project, outlines design and development process.”.
- [2] “Parachute descent rate calculator.” https://fruitychutes.com/help_for_parachutes/parachute-descent-rate-calculator.htm, Accessed 3 March 2018.
- [3] A. M. Kuethe and C.-Y. Chow, Foundations of Aerodynamics. John Wiley and Sons, Inc, 5 ed., 1998.
- [4] Z. Howard, “How to calculate fin flutter speed,” Peak of Flight, July 2011.
- [5] K. J. Astrom and R. M. Murray, Feedback Systems, pp. 7.1–7.35. Princeton University Press, October 2016.
- [6] F. Zheng-ping, Z. Ji-mao, and R. Allen, “Design of continuous and discrete lqi control systems with stable inner loops,” Journal of Sjamgjao Jiaotong University, vol. E-12, no. 6, pp. 787–792, 2007.
- [7] International Conference on Informatics in Control, Automation, and Robotics, Iterative linear Quadratic Regulator Design for Nonlinear Biological Movement Systems.
- [8] P. D. Groves, Principles of GNSS, Inertial, and Multisensor Integrated Navigation Systems. Artech House, 2008.
- [9] J. L. Crassidis and J. L. Junkins, Optimal Estimation of Dynamic Systems. Boca Raton, FL : CRC Press, 2 ed., 2012.

- [10] D. Gebre-Egziabher and G. H. Elkaim, “Mav attitude determination by vector matching,” *IEEE Transactions on Aerospace and Electronic Systems*, vol. 44, pp. 1012–1028, July 2008.
- [11] R. W. Beard, *Small Unmanned Aircraft: Theory and Practice*, pp. 254–259. Princeton University Press, 2012.